Carbon-steel tube surface mounted FBG sensors under high-temperature environment, part I: Polyimide coated and femtosecond laser written

Aayush MADAN[1,2], Ouyang LIU[2], Wenyu JIANG[2], Yixin WANG[2], Perry Ping SHUM*[1], and Jianzhong HAO[2]

[1]School of Electrical and Electronic Engineering, Nanyang Technological University, Singapore 639798
[2]Institute for Infocomm Research, Agency for Science, Technology and Research, Singapore 138632
*Corresponding author: Shum@ieee.org

***Abstract*— Fiber Bragg Grating (FBG) sensors need to be mounted at the outer surface of any metallic test piece to monitor its structural integrity through measuring physical quantities, such as strain, pressure, vibration, and temperature. High-temperature epoxies or ceramic epoxies are used to mount the said sensors to operate under high-temperature environment conditions. The unsteadiness of the outer surface of the metallic piece and non-uniformity of the applied epoxy over the sensing head, affect its operation and measurement accuracy in the long run. Here, in the first part of a two-part article, we have investigated the reliable functioning and spectrum evolution of the FBG sensors, mounted on a carbon-steel tube, for temperature up to 500°C. Polyimide coated femtosecond laser written FBG sensors are surface mounted on the said tube using a high-temperature adhesive. There is no peak splitting, and chirp phenomenon experienced by the sensors at the end of two thermal cycles. The second part of the two-part article focuses on the mounting and operation of gold-coated FBG sensors in the high-temperature operating environment.**

***Index Terms*— optical fiber sensors; FBG sensors; High-temperature sensor mounting; steel tube; temperature monitoring.**

I. Introduction

Fiber optic (FO) sensors are replacing traditional electric sensors in many applications because FO sensors typically offer long lasting sensing solution for harsh conditions, provide more reliable data, being compact and light weight [1]. The FBG sensors have the capability to be embedded underneath metallic structures and controlling the structure health parameters [2], hence provide a useful monitoring mechanism in a challenging environment. The applicability of FBG sensors in high temperature operating environment requires a different mechanism of grating formation i.e., Type II, regenerated, or femtosecond laser written gratings [3], [4], etc. FO sensors are also attractive as pressure sensors and in arrays with many temperature sensing points [5]. The typical applications of FO sensors include, but not limited to, security, oil and gas, power, healthcare, civil structure health monitoring, transportation and aerospace industries, [6]–[10]. In principle, an FBG is a periodic perturbation of refractive index in the core of an optical fiber along the longitudinal central axis, as shown in fig. 1, causing reflection of the resonating wavelength within the optical fiber [8], [11].

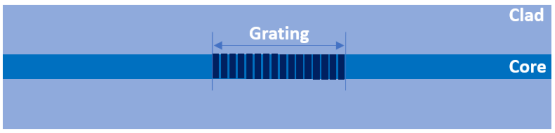

Fig. 1: Schematic structure of an FBG

All the resonant wavelengths satisfy the Bragg condition [12] given by eq. (1).

$$\lambda_B = 2n_{eff}\Lambda \tag{1}$$

where λ_B is the Bragg wavelength, n_{eff} is the effective refractive index, and Λ is the period (or pitch) of grating.

The structure also behaves as an optical band rejection filter by transmitting non-resonating wavelengths [13]. The wavelength of maximum reflection does not only depend on grating period but also on temperature and strain [14] as in eq. (2), where C_s and C_t are the coefficient of strain and temperature, respectively. Symbols ξ and $\triangle$T represent the applied strain and change in temperature, respectively.

$$\frac{\triangle \lambda_B}{\lambda_B} = C_s.\xi + C_t.\triangle T \tag{2}$$

Therefore, the grating structure can be used as a direct sensor for measurement of temperature and/or strain, and as a transduction element for other measurands. Overall, the technique is becoming popular for structure health or integrity monitoring in various applications worldwide.

The FBG sensors are durable till the temperature at which the grating gets erased which depends on the fiber material and grating writing technique. At higher temperatures, the FBG undergo transformations, i.e., the grating gets erased affecting its optical response and ruining the calibration. Other causes for the grating decay include thermal expansion, dopant migration, silica devitrification, and thermic optic delay [15].

Monitoring of physical quantities, such as temperature and strain at the outer surface of any metallic piece, especially when the operating environment is experiencing temperature

ranging 400-500°C, is still a challenge for many applications. Therefore, for such applications the mounting and packaging of the FBG sensors become more crucial for robust operation in a longer run.

In this paper, we have investigated the response of femtosecond laser written polyimide coated FBG sensors, surface-mounted on a carbon-steel tube for up to 500°C. There is no peak splitting, and chirp phenomenon experienced by the sensors at the end of two thermal cycles.

II. Sensor Consideration

The ultrafast pulse lasers have opened a new door of exploration and application of optical FBG sensors. The grating structures inscribed using femtosecond lasers have attractive annealing characteristics and may provide a long-term stable operation in high-temperature environment than conventional ultra-voilet (UV) laser written grating structures. Therefore, femtosecond laser written sensors are far more suitable candidate for applications, including but not limited to, aerospace and automobile applications, well and pipeline monitoring, wind turbine, distributed temperature sensing, exhaust control, smart structures, and power plant control, etc. [16]. Another advantage of femtosecond laser inscription is that the fiber does not need to be photo sensitive [17]–[20] as refractive index changes are initiated by a multi photon process.

A short length grating with well-defined spectra can be used as miniaturized distributed strain sensors which also provides small form factor packaging with low insertion loss for distributed monitoring [21]. When the length of an FBG is longer and such FBG is attached to a curved surface, as in our experimental study, the grating pitch become uneven due to non-uniform stress distribution along the grating length.

This unevenness of the grating pitch may cause chirp causing peak splitting in the wavelength spectrum which makes the signal processing more tedious [22] as the detection of the reflected peak wavelength becomes more complicated. Different peak-detect algorithms may result in various wavelength readings, hence the derived values of the measurand. Therefore, a shorter FBG length is used to minimize the chirp effect caused by non-uniform stress distribution along the grating length.

FBGs coated with the polymer of imide monomers have a reliable performance for temperature up to 350°C. With femtosecond laser, grating is written without removing the coating which comes out to be a permanent grating to ensure ample annealing characteristics and better thermal stability.

III. Experimental Set Up

This section emphasizes on the experiment which is carried out first by mounting the two designed polyimide coated femtosecond laser written FBGs onto a carbon steel tube, followed by two heating and cooling cycles from room temperature to 500°C, as shown in the set-up, Fig. 2.

At first, the tube is surface treated to remove passive layer and rust before mounting the sensors. Brushing a primer layer of the resin ensures the penetration in small defects,

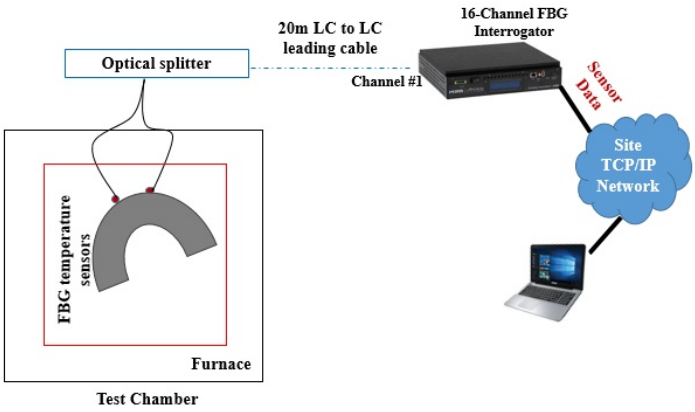

Fig. 2: Experimental set up

if present after the treatment. Next, the sensors are mounted using high-temperature adhesive resins and are to be cured using a proper curing procedure before the actual testing. Afterwards, the tube is placed inside a furnace to undergo the high-temperature test, i.e. from room temperature to 500°C with a certain, maintain at maximum temperature for an hour, followed by cooling down, as shown in Fig. 3. The sensors are connected to an interrogator system through an optical splitter, as in Fig. 2, to capture the sensor data during the test.

IV. Results and Discussions

We have investigated the response of the sensors in terms of their peak reflection wavelength and reflection spectrum evolution under both the thermal cycles (cycle 1 and 2).

A. Wavelength response to temperature

The analysis of the wavelength shift to temperature is performed to understand how the mounted sensors are behaving with respect to different temperature. Furthermore, it helps to understand the relaxation behaviour of the sensor. The wavelength shift of both the FBG sensors is shown in Fig. 4, along with variation of temperature at y2 axis. Both the sensors follow the temperature profile. Following are the heating and cooling phase under both the thermal cycles:

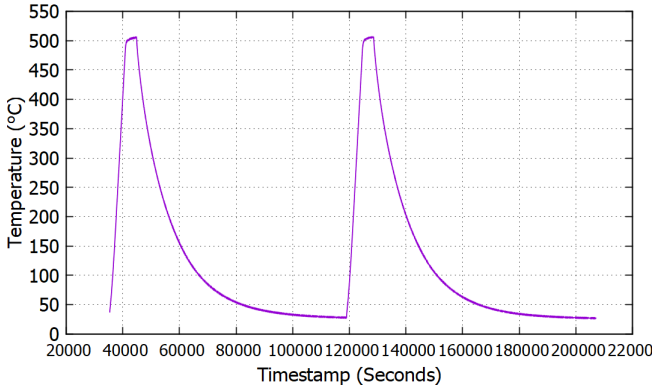

Fig. 3: Thermal cycles

- Heating and Cooling under first thermal cycle

The wavelength response of the sensors during heating and cooling, under first thermal cycle is shown in Fig. 5a. The FBG1 and FBG2 follow the following linear fitting equations, eq. (3) and (4), respectively.

$$Y = 1529.306 + (0.0145)X \tag{3}$$

$$Y = 1544.130 + (0.0145)X \tag{4}$$

Once the furnace temperature reaches at the highest set-point, i.e. 500°C, it is maintained for one hour before dropping down naturally. The wavelength response of the sensors during heating and cooling, under second thermal cycle is shown in Fig. 5b. The FBG1 and FBG2 follow the linear fitting equations, given by eq. (5) and (6), respectively. The sensor's sensitivity reduces slightly to 12 pm/°C.

$$Y = 1529.84 + (0.0123)X \tag{5}$$

$$Y = 1544.692 + (0.0124)X \tag{6}$$

- Heating and Cooling under second thermal cycle

After completing the first thermal cycle, the furnace temperature is again ramped up to 500°C and cooled down naturally to room temperature, i.e. another consecutive cycle. The wavelength response of the two FBG sensors for the second thermal cycle is shown in Fig. 6a and 6b. The response of the two sensors follows eq. (7) and (8) respectively for heating up, and (9) and (10) respectively for cooling down, with sensing sensitivity remains stable at 12 pm/°C.

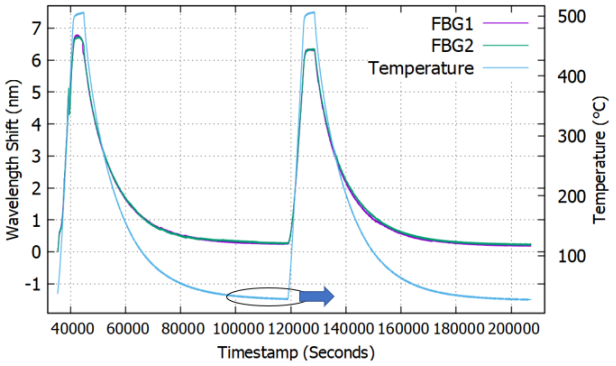

Fig. 4: FBG wavelength shift and temperature variation

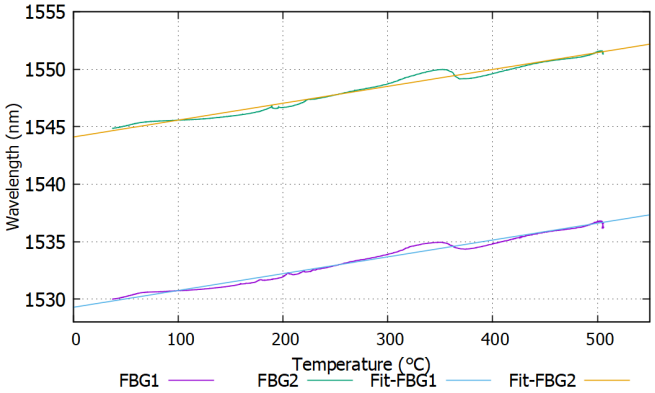

(a) Response during heating

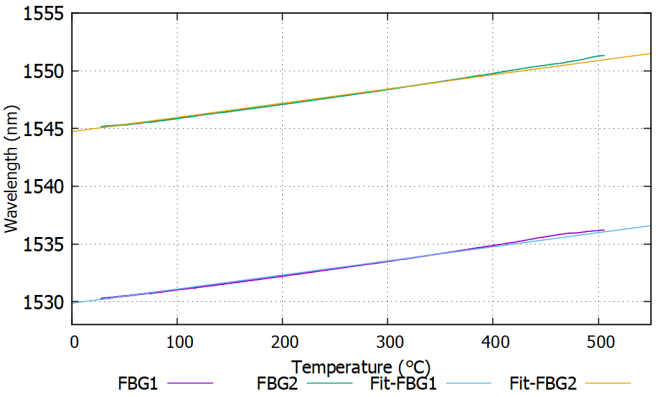

(b) Response during cooling

Fig. 5: Response under first thermal cycle

TABLE I: Pearson Correlation Summary between Sensor response and Temperature

Cycle	FBG1	FBG2
Cycle 1: Heating	0.995	0.994
Cycle 1: Cooling	0.998	0.998
Cycle 2: Heating	0.995	0.996
Cycle 2: Cooling	0.998	0.998

$$Y = 1529.619 + (0.0122)X \tag{7}$$

$$Y = 1544.498 + (0.0122)X \tag{8}$$

$$Y = 1529.791 + (0.0123)X \tag{9}$$

$$Y = 1544.684 + (0.0125)X \tag{10}$$

B. Spectral response to temperature

Following describes evolution of the reflection spectrum of both the sensors during the second thermal cycle. From the Fig. 7 and 8, it is observed that the spectrum experiences

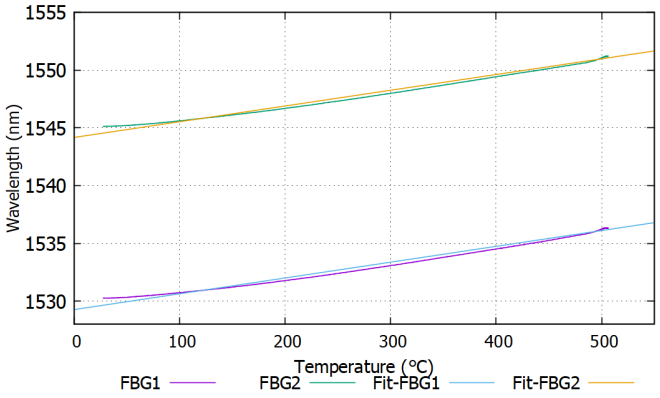

(a) Response: heating up second cycle

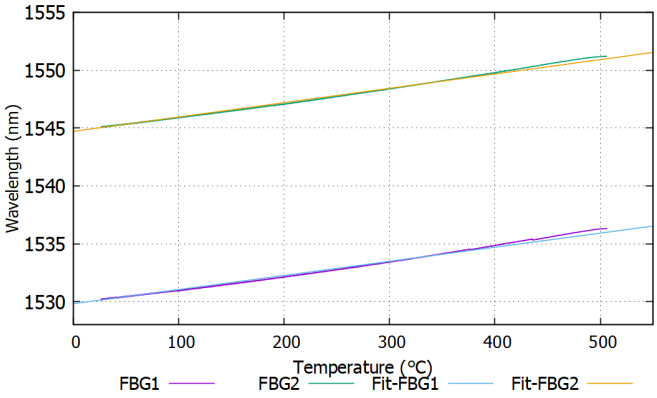

(b) Response: cooling down second cycle

Fig. 6: Response under second thermal cycle

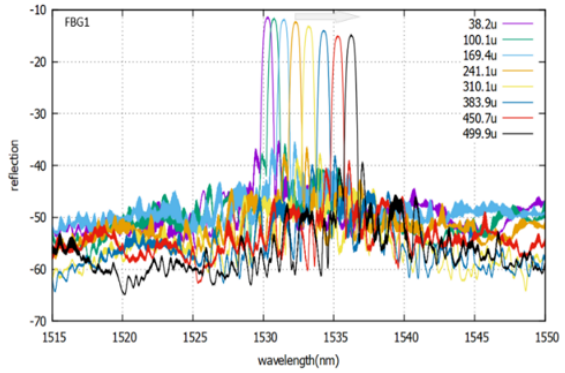

(a) FBG1: heating second cycle

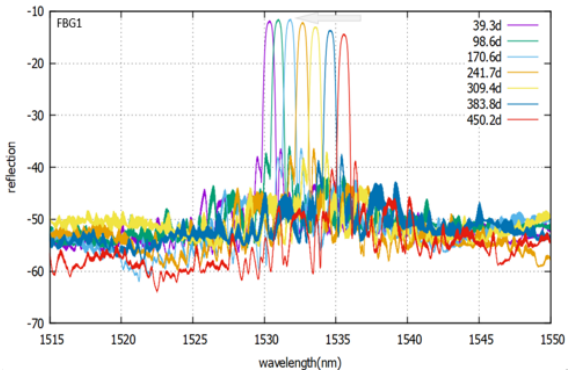

(b) FBG1: cooling second cycle

Fig. 7: Spectrum evolution of FBG1

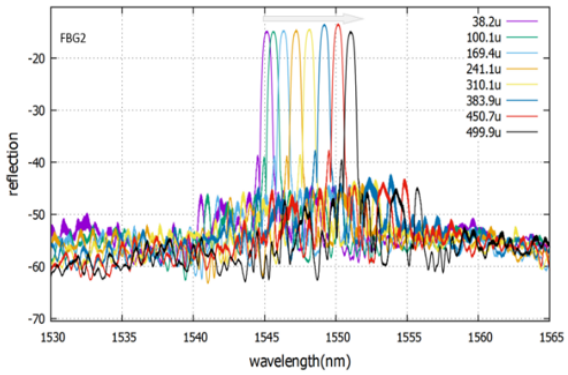

(a) FBG2: heating second cycle

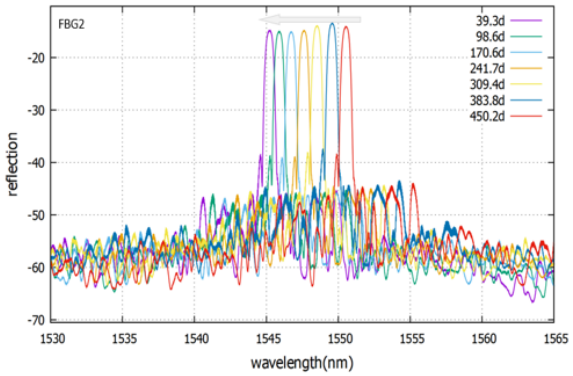

(b) FBG2: cooling second cycle

Fig. 8: Spectrum evolution of FBG2

red shift during heat up and blue shift during cool down. The spectrum remains consistent without experiencing any splitting or broadening in the reflected peak. In the identification of lines in graphs, numbers represent the temperature at that spectrum, the 'u' and 'd' in the curve refer to increase and decrease in temperature, respectively.

V. CONCLUSIONS

After the experiment, we observed that both the FBG sensors survive the 500°C temperature range and have a linear wavelength response to the temperature. None of the sensor experiences chirp or peak splitting in its reflection spectrum throughout the temperature range. And, it has also been witnessed that the fiber become very fragile and loses its mechanical strength because the polyimide coating evaporates after experiencing such temperature.

Therefore, the sensors are suitable for mounting on the surface of such carbon steel tubes operating in high-temperature environment, provided there's a mean of outer metal coating present on the optical fiber to increase its mechanical strength and robustness in such environment. Next, in part II of this article, we will present mounting and testing of gold coated fiber sensors on a carbon steel tube for repeated cycles.

ACKNOWLEDGMENT

This work was supported by the National Research Foundation (NRF) Singapore, Energy Innovation Research Programme, under its Sembcorp-EMA Energy Technology Partnership (SEETP) (Singapore, LA/ Contract No: NRF2015EWT-EIRP001-010) and Ministry of Education - Singapore, Academic Research Fund Tier 1 (MOE2019-T1-001-111). The authors would like to thank Keng Boon Siah, Kheong Keng Tan, and Karan M Sabnani at Sembcorp Industries Ltd Singapore, for their domain knowledge and suggestions. The authors would also like to thank Gabriel Loh, Maryanne Toh, and Regina Low at the Institute of

Chemical and Engineering Sciences Limited, under Agency for Science, Technology, and Research Singapore, for providing access to their research labs and helping to conduct the experiment.

REFERENCES

[1] Hochberg, R.C., *Fiber-optic sensors*. IEEE Transactions on Instrumentation and Measurement, 1986. IM-35(4): p. 447-450.

[2] Madan, A., et al. Fiber Bragg grating sensors for real-time monitoring of boiler U-bend tubes thinning. in 2017 Conference on Lasers and Electro-Optics Pacific Rim (CLEO-PR). 2017.

[3] Madan, A., et al. Sensing Characteristics of a Grating-Based Fabry-Perot Structure in a Biconical Tapered Fiber. in 2019 IEEE 4th Optoelectronics Global Conference (OGC). 2019.

[4] Madan, A., et al., Investigation of a Bragg Grating-Based Fabry–Perot Structure Inscribed Using Femtosecond Laser Micromachining in an Adiabatic Fiber Taper. Applied Sciences, 2020. 10(3).

[5] Wang, C., et al. Temperature Sensor Based on Selectively Liquid Infiltrated Dual Core Photonic Crystal Fiber. in 2019 IEEE Photonics Conference (IPC). 2019.

[6] Ahmad, H., et al., *High Sensitivity Fiber Bragg Grating Pressure Sensor Using Thin Metal Diaphragm*. IEEE Sensors Journal, 2009. 9(12): p. 1654-1659.

[7] Chan, P.K.C., et al., *Multi-point strain measurement of composite-bonded concrete materials with a RF-band FMCW multiplexed FBG sensor array*. Sensors and Actuators A: Physical, 2000. 87(1): p. 19-25.

[8] Jung, J., et al., *Fiber Bragg grating temperature sensor with controllable sensitivity*. Applied Optics, 1999. 38(13): p. 2752-2754.

[9] Xiang Kai, Z. and R. Yun Jiang, *Simultaneous Static Strain, Temperature and Vibration Measurement Using an Integrated FBG/EFPI Sensor*. Chinese Physics Letters, 2001. 18(12): p. 1617-1619.

[10]] Zhuo, Z.C. and B.S. Ham, *A temperature-insensitive strain sensor using a fiber Bragg grating*. Optical Fiber Technology, 2009. 15(5): p. 442-444.

[11] Sipe, J.E., L. Poladian, and C.M. de Sterke, *Propagation through nonuniform grating structures*. Journal of the Optical Society of America A, 1994. 11(4): p. 1307-1320.

[12] Pashotta, R., *Fiber Bragg Gratings*, in RP Photonics: Encyclopedia of Laser Physics and Technology.

[13] Mihailov, S.J., *Fiber Bragg Grating Sensors for Harsh Environments*. Sensors, 2012. 12(2): p. 1898-1918.

[14] Andreas, O. and K. Kyriacos, *Fiber Bragg Gratings: Fundamentals and Applications in Telecommunications and Sensing*. Artech House Optoelectronics Library. 1999: Artech House Print on Demand. 433.

[15] Adamovsky, G., et al., *Fiber Bragg Based Optical Sensors for Extreme Temperatures*, in Infotech@Aerospace 2011. 2011, American Institute of Aeronautics and Astronautics.

[16] FemtoFiberTecGmbH, *Femtosecond-laser-written Fiber Bragg Gratings for Smart Sensing Solutions*. 2013.

[17] Liao, C.R. and D.N. Wang, *Review of femtosecond laser fabricated fiber Bragg gratings for high temperature sensing*. Photonic Sensors, 2013. 3(2): p. 97-101.

[18] Florea, C. and K.A. Winick, *Fabrication and characterization of photonic devices directly written in glass using femtosecond laser pulses*. Journal of Lightwave Technology, 2003. 21(1): p. 246-253.

[19] Gattass, R.R. and E. Mazur, *Femtosecond laser micromachining in transparent materials*. Nature Photonics, 2008. 2: p. 219.

[20] Mihailov, S.J., et al., *Bragg gratings written in all-SiO/sub 2/ and Ge-doped core fibers with 800-nm femtosecond radiation and a phase mask*. Journal of Lightwave Technology, 2004. 22(1): p. 94-100.

[21] Meng-Chou, W., R.S. Rogowski, and K.K. Tedjojuwono. *Fabrication of extremely short length fiber Bragg gratings for sensor applications*. in SENSORS, 2002.

[22] Li, B., et al. Robust Convolutional Neural Network Model for Wavelength Detection in Overlapping Fiber Bragg Grating Sensor Network. in 2020 Optical Fiber Communications Conference and Exhibition (OFC). 2020.